

Why Pre-trained Models Fail: Feature Entanglement in Multi-modal Depression Detection

Xiangyu Zhang, Beena Ahmed *Member, IEEE*, Julien Epps *Senior Member, IEEE*

Abstract—Depression remains a pressing global mental health issue, driving considerable research into AI-driven detection approaches. While pre-trained models, particularly speech self-supervised models (SSL Models), have been applied to depression detection, they show unexpectedly poor performance without extensive data augmentation. Large Language Models (LLMs), despite their success across various domains, have not been explored in multi-modal depression detection. In this paper, we first establish an LLM-based system to investigate its potential in this task, uncovering fundamental limitations in handling multi-modal information. Through systematic analysis, we discover that the poor performance of pre-trained models stems from the conflation of high-level information, where high-level features derived from both content and speech are mixed within pre-trained models model representations, making it challenging to establish effective decision boundaries. To address this, we propose an information separation framework that disentangles these features, significantly improving the performance of both SSL models and LLMs in depression detection. Our experiments validate this finding and demonstrate that the integration of separated features yields substantial improvements over existing approaches, providing new insights for developing more effective multi-modal depression detection systems.

I. INTRODUCTION

Depression is a widespread mental health disorder, impacting 10-15% of the global population and marked by persistent low mood, diminished interest and fatigue, making it a significant and costly health challenge [1]. Traditional methods for diagnosing and treating depression are often resource-intensive and may lack efficacy, leading researchers to increasingly focus on developing automated systems for depression detection. Pre-trained models, particularly speech self-supervised models (SSL Models), have emerged as promising tools for this task, given their ability to learn from limited labeled data [2], [3]. However, these models consistently show poor performance in multi-modal depression detection without extensive data augmentation [4], [5], raising fundamental questions about their limitations in this critical healthcare application.

This unexpected failure of pre-trained models in depression detection leads to our primary research questions: (1) Why do SSL models, despite their proven effectiveness across various speech tasks, perform poorly in depression detection? (2) What are the fundamental challenges in combining speech and text modalities for depression detection? (3) How can we design a system that effectively addresses these limitations without relying on extensive data augmentation?

Xiangyu Zhang, Beena Ahmed, Julien Epps are with the School of Electrical Engineering and Telecommunications, University of New South Wales, Sydney, Australia.

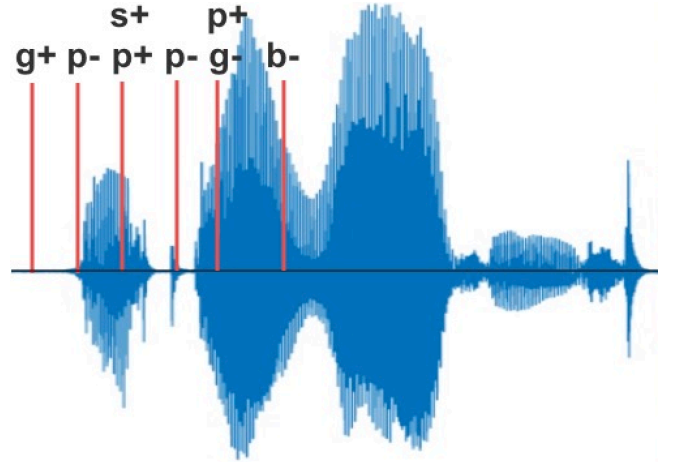


Fig. 1: Example of acoustic landmarks (2-gram landmarks (g+p-), (s+p+), (p-,p+), ..., (g-b-)). Landmarks can discretize speech into a series of tokens.

To systematically investigate these challenges, we turn to another type of pre-trained model - Large Language Models (LLMs), which have recently demonstrated unprecedented capabilities in understanding complex patterns and generalizing across domains [6], [7]. As the most advanced pre-trained models to date, LLMs have shown remarkable success in various healthcare applications [8], [9], [10] and could potentially capture subtle linguistic patterns that might indicate depression. To enable this investigation, we develop a system that integrates speech information through acoustic landmarks - discrete markers capturing temporal speech patterns [11], [12], [13]. These landmarks provide an efficient alternative to memory-intensive continuous representations, making them well-suited for integration with LLMs.

However, our systematic investigation reveals that even these powerful models struggle with multi-modal depression detection, suggesting a more fundamental issue than model capacity or architecture. This observation leads to our core hypothesis: the challenge lies in how these pre-trained models internally represent and process multi-modal information, **where the conflation of high-level features derived from both content and speech creates confused decision boundaries**. Traditional approaches have attempted to improve performance through extensive data augmentation [4], [14], but this workaround fails to address the underlying problem and contradicts the intended purpose of pre-trained models - to generalize effectively with limited labeled data.

Based on this hypothesis, we propose an information

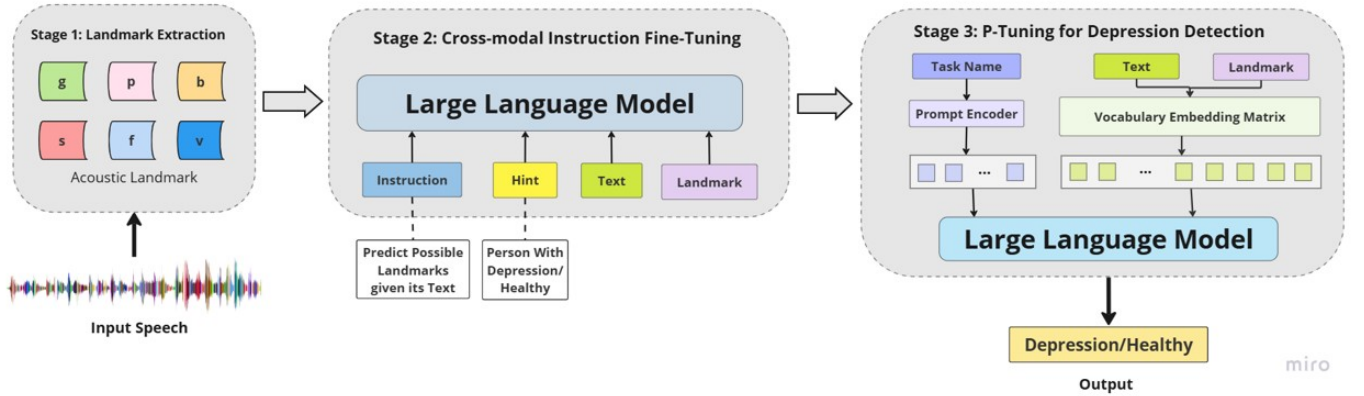


Fig. 2: Overview of the proposed LLM-landmark depression detection baseline system, broadly categorized into three stages: landmark detection (on the left), cross-modal instruction fine-tuning (in the middle), and P-tuning for depression detection (on the right).

separation framework that deliberately disentangles content-specific and speech-specific features. This approach represents a fundamental shift from previous methods that attempt to combine modalities directly. Our experimental results validate this hypothesis, demonstrating that separated, specialized representations significantly outperform traditional approaches without relying on data augmentation. Moreover, by integrating our speech dense vectors (designed to capture only speech-specific information) with the LLM embeddings, we achieve substantial improvements in LLM-based depression detection system. This result confirms that while content and speech information in speech SSL Models should be processed separately, they can be highly complementary when properly integrated, leading to good performance in multi-modal depression detection.

The remainder of this paper is organized as follows. Section III presents our initial LLM-based system we published previously [14] and its limitations, Section IV analyzes why pre-trained models fail in depression detection, Section V introduces our information separation framework, and Section VI, VII details the experimental results and analysis.

II. RELATED WORK

A. Acoustic Landmarks

The concept of acoustic landmarks has its roots in studies of distinctive features [15], [12]. Some researchers suggest that for certain phonetic distinctions, listeners depend on acoustic landmarks to capture essential cues necessary for interpreting the associated distinctive features [11]. This view underscores the significance of landmarks in auditory perception and speech comprehension. Over time, acoustic landmarks have found applications not only in speech recognition [11], [16] but also in addressing issues related to mental health [17], [18]. Although definitions of acoustic landmarks vary somewhat across studies, Boyce et al. [19] extended Liu’s earlier work [11] by introducing a MATLAB-based landmark detection toolkit (SpeechMark), which has since become one of the most widely utilized resources for landmark technology.

B. Depression Detection

AI technology has been employed in automatic depression detection for several years, beginning with traditional

approaches like Support Vector Machines (SVMs) [20], as investigated by Cummins and others [21], [17], [18]. With advancements in deep learning [22], [23], researchers have increasingly adopted deep learning methods for this task. Zhao et al. have explored transformer models for processing speech in depression detection [24], while Shen and colleagues utilized BI-LSTM architectures to integrate text and speech inputs [25]. Building on these methods, Wu [4] implemented speech self-supervised models [3], [26], [27] and integrated them with RoBERTa [28], creating a more comprehensive multimodal framework that combines both text and audio for depression detection.

C. Parameter-Efficient Fine-tuning

Parameter-efficient fine-tuning (PEFT) methods have gained significant attention as alternatives to full model fine-tuning, particularly for large pre-trained models. LoRA [29] introduces low-rank adaptation matrices to modify key weight matrices during fine-tuning while freezing the original model parameters. Prefix tuning [30] prepends trainable continuous tokens to the input, allowing task-specific adaptation without modifying the model architecture. P-tuning [31] extends this concept by introducing trainable prompts at different layers of the model. These approaches have demonstrated comparable performance to full fine-tuning while requiring significantly fewer trainable parameters. For multimodal tasks, BitFit [32] showed that adapting only bias terms can effectively transfer pre-trained models across modalities.

III. BASELINE SYSTEM

Our methodology, shown in Figure 2, follows a structured three-phase approach. In the first phase, we extract acoustic landmarks from speech and perform various data processing techniques. The next phase, cross-modal instruction fine-tuning, involves guiding the LLM to learn the specific characteristics and nuances of these acoustic landmarks. In the final phase, P-Tuning, the LLM is refined to apply this understanding effectively for depression diagnosis.

TABLE I: Descriptions of the Six Investigated Landmarks

Landmark	Description
p	Start (+) or end (-) of periodicity
v	Onset (+) or offset (-) of voiced frication
s	Release (+) or closure (-) of a nasal
f	Onset (+) or offset (-) of frication
g	Start (+) or end (-) of vocal fold vibrations
b	Onset (+) or offset (-) of turbulent noise during obstruent regions

A. Landmark Extraction

Figure 1 illustrates acoustic landmarks as a discretization of speech signals into acoustic tokens. Our study utilizes a Python-based landmark detection algorithm, which builds on the approaches of Liu [11] and Boyce [19]. The detection process begins by dividing the spectrogram into six frequency bands, where energy shifts are analyzed in two detection stages to identify specific landmarks. For **glottal (g)** landmarks, marking the onset and offset of vocal fold vibrations, we monitor low-frequency bands for abrupt energy increases or decreases exceeding a 5 dB threshold. To capture physiological accuracy, we ensure each glottal onset has a corresponding offset using dynamic programming, reflecting natural glottal cycles. **Burst (b)** landmarks, associated with plosive sounds, are detected through sharp energy increases in the mid-frequency bands, using an 8 dB threshold to differentiate bursts from other acoustic events. Syllabic regions, represented by **syllabic (s)** landmarks, are identified based on gradual energy buildup or drop within the mid to high-frequency bands, with a 6 dB threshold used to capture sustained energy characteristic of vowels or sonorant consonants.

Further, to detect **frication (f)** and **voiced Friction (v)** landmarks, we examine power shifts within the high-frequency bands and adjust energy levels in the low-frequency bands to differentiate fricative sounds in unvoiced and voiced regions. For detecting **periodicity (p)** landmarks, autocorrelation calculations are applied to audio frames, capturing recurring patterns indicative of voiced speech. Finally, to address data limitations, we augment the dataset by sampling sub-dialogues, balancing depression cases, and leveraging consecutive landmark pairs to efficiently represent the sequence of acoustic events in each speech segment. This method captures essential acoustic and timing information necessary for effective analysis in depression detection tasks.

B. Data Augmentation

Clinical depression assessments typically involve assigning a single label to each session conducted through interviews. This labeling, when applied to a fixed dataset, results in fewer samples compared to the abundant utterances and frames available in other speech tasks, creating challenges of data scarcity. Additionally, severe data imbalance persists, as healthy cases (positive) are significantly fewer than depression cases (negative). To address this, we adopted the sub-dialogue shuffling approach from Wu et al. [4], sampling segments

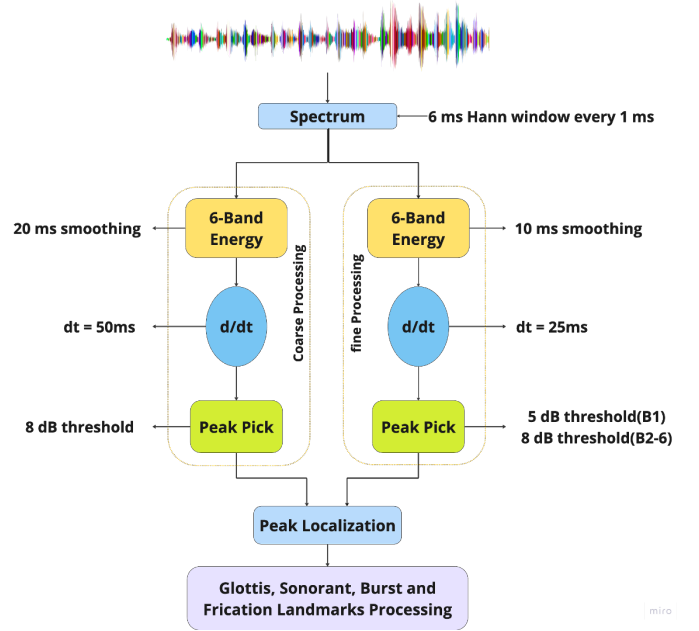


Fig. 3: Landmark Detection System

$x_{s:e}$ from complete dialogues $x_{1:T}$, with s and e indicating random start and end utterances.

Using acoustic landmarks enables us to extend the sub-dialogue length beyond traditional frame-based approaches while maintaining computational efficiency. We maintain dataset consistency with Wu’s method by using 1,000 sub-dialogue samples ($M=1000$). Building on prior findings that landmark patterns are more informative than individual landmarks [18], we group consecutive landmark pairs to capture richer temporal patterns while reducing sequence length, as illustrated in Figure 1.

C. Hint Cross-modal Instruction Fine-Tuning

Our approach begins by equipping the LLM with an understanding of acoustic landmarks, an essential step since LLMs are not natively exposed to this type of data. This foundational training enables the model to recognize, interpret, and utilize acoustic landmark information effectively.

In the central part of Figure 2, we illustrate our method, which involves instructing the LLM to predict probable acoustic landmarks based on textual input. This process serves two purposes: it familiarizes the LLM with acoustic landmarks and establishes a connection between the speech (landmarks) and text modalities through paired data. To achieve efficient adaptation, we incorporate low-rank matrices into the Query and Key matrices of the self-attention layer via LoRA [29]. We also adjust the embedding layer to accommodate the newly integrated landmarks in the vocabulary. Throughout training, we update the **embedding layer**, **linear head**, and **LoRA matrices** to ensure the effective integration of landmark features. The objective is to minimize the negative log-likelihood across all samples, including the prefix, expressed as:

$$\mathcal{L}(M|C) = - \sum_{j=1}^x \sum_{i=1}^{y_j} \log P(s_{i,j} | s_{<i,j}, M), \quad (1)$$

where x represents the dataset sample count C , y_j corresponds to text with associated landmarks in each sample S , and M is the fine-tuned language model.

Our cross-modal instruction fine-tuning process incorporates contextual hints about the depression status of the speakers. Experimental results show that these hints significantly improve the LLM’s performance in depression detection. This improvement in performance when provided with depression-related context suggests that acoustic landmarks indeed capture diagnostically relevant patterns - an observation that aligns with prior findings about the relationship between speech patterns and depression [33], [18].

D. P-Tuning for Depression Detection

In the initial phase, we trained the LLMs to comprehend the concept of landmarks. Building on this foundation, we applied P-tuning [31] to enable the LLMs to integrate both text and landmark information for effective depression detection. For this purpose, we replaced the language modeling head with a classification layer. The training objective was to minimize the cross-entropy loss for classification, represented as:

$$\mathcal{L} = - \sum_{c=1}^C y_{o,c} \log(p_{o,c}), \quad (2)$$

where C is the total number of classes, $y_{o,c}$ serves as an indicator variable set to 1 if the observation o belongs to class c , and 0 otherwise. $p_{o,c}$ denotes the predicted probability that observation o falls within class c .

Our experiments with different fine-tuning approaches revealed that directly applying LoRA across all layers of Llama2 yielded better performance than using manual templates with P-tuning. Based on these findings, we adopted the full-layer LoRA approach for our subsequent experiments with the baseline system.

E. Baseline Experimental Setup

Dataset. The DAIC-WOZ dataset [34] is widely regarded as a benchmark for multimodal depression detection, comprising 189 recorded clinical interviews between interviewers and patients. In the training set, 30 out of 107 interviews are marked as depressed, while the development set includes 12 cases of depression among 35 interviews. Consistently with previous studies [35], [25], [36], [4], we evaluated our results using the development subset. **Model Configurations.** Our experiments employed the Llama2-7B, Llama-7B Chat, Llama2-13B, and Llama2-13B Chat models [7], conducted on a system with 8 NVIDIA A100 80GB GPUs. The Llama 2-Chat models were tailored for interactive, conversational tasks. During the cross-modal instruction fine-tuning stage, we fine-tuned the model for 10 epochs with a batch size of 128, LoRA rank of 8, 100 warmup steps, and a learning rate of 1e-6. For the depression detection phase, we fine-tuned the model over 8 epochs with a batch size of 256, 30 virtual tokens, 256 encoder hidden units, and a learning rate of 1e-6. In both phases, AdamW served as the optimizer, and model parallelism was implemented to facilitate efficient fine-tuning. In the ablation study, we applied hyperparameter tuning using the Tree-structured Parzen Estimator (TPE) method [37].

TABLE II: F1 scores across LLM and speech models by input type. Text-based, landmark-based, and combined inputs were evaluated on various LLM configurations, with Speech SSL models (with data augmentation) included for comparison.

Input Type	Model	F1 Score
Text	Llama2-7B	0.578
	Llama2-7B Chat	0.488
	Llama2-13B	0.636
	Llama2-13B Chat	0.545
Zero Shot-Text	GPT-3.5	0.545
	GPT-4	0.571
Landmark	Llama2-7B	0.521
	Llama2-7B Chat	0.434
	Llama2-13B	0.559
	Llama2-13B Chat	0.538
Text + Landmark	Llama2-7B	0.545
	Llama2-7B Chat	0.500
	Llama2-13B	0.695
	Llama2-13B Chat	0.666
Speech SSL Models [4]	Wav2vec 2.0	0.627
	HuBERT	0.667
	WavLM	0.700

F. Baseline Comparison with Previous Pre-trained Model Results

Table II summarizes the F1 scores achieved by Llama2 models across various configurations for depression detection, while also comparing these results with those of GPT-3.5 and GPT-4 in the text-only modality. Notably, GPT-3.5 and GPT-4 were not fine-tuned specifically for this task; rather, we utilized meticulously designed prompts to guide the models in evaluating whether each sample originated from a patient with depression.

For the ‘landmark’ and ‘text + landmark’ modalities, our process first entailed cross-modal instruction fine-tuning with hints, followed by P-tuning to optimize for depression detection. This approach aimed to equip the LLMs with a foundational understanding of landmarks before advancing to the diagnostic stage.

The findings show that LLMs relying solely on text for depression detection yield relatively modest performance across all models, even including state-of-the-art models like GPT-3.5 and GPT-4, which typically excel in various applications. This performance shortfall can be attributed to two primary factors. Firstly, **text alone is limited in conveying emotional context**, as it lacks the nuances found in speech. For example, the phrase “It’s raining today” might evoke a positive sentiment for some while a negative sentiment for others. Although text alone leaves these interpretations ambiguous, speech data could capture the emotional tone more accurately. Secondly, **data constraints also impact model performance**. Labels are assigned only at the document level, and there are limited data samples available currently, since there is no large public dataset for multimodal depression detection. These factors, combined with the lack of data granularity, restrict the model’s capacity for accurate detection.

Integrating landmarks improved the performance across all

TABLE III: Average and Maximum F1 Scores for Wav2Vec, WavLM, and HuBERT at Specific Layers with SVM classifier

Model	Layer	Average F1	Max F1
Wav2Vec 2.0	8	0.597525	0.625
WavLM	8	0.6471	0.6471
HuBERT	10	0.5707	0.6286

models, validating the benefit of incorporating landmark-based information. Landmarks convey affective variations, embedding additional acoustic information that aids LLMs in identifying depression. However, relying solely on landmarks remained suboptimal for depression detection, likely due to the fact that even after cross-modal fine-tuning, integrating information exclusively from other modalities (like audio or visual) can reduce the stability of LLMs [38], [39].

IV. CURRENT LIMITATIONS AND DISCUSSION

A. Limitations of Pre-trained Models in Depression Detection

Existing methods for depression detection using LLMs and speech SSL models generally rely on data augmentation to increase dataset size, as shown in Table II. This approach contradicts the foundational aim of SSL models, which are designed to generalize across a variety of downstream tasks with minimal labeled data. Table III shows the performance of speech SSL models on depression detection without data augmentation. We selected the best-performing layer based on previous studies [4] and conducted experiments on the development set to ensure fair comparisons and thorough analysis. Using random hyperparameter search, we report both the average and maximum F1 scores achieved, applying the same methodology in subsequent experiments.

As seen in Table III, the absence of data augmentation results in a notable decline in performance for speech SSL models in the depression detection task. Additionally, information in speech SSL models is distributed across multiple layers [3], [26], highlighting the limitations of relying solely on a single layer for this purpose.

Shifting the focus to LLMs, their application to depression detection presents a distinct set of challenges. Specifically, LLMs also require data augmentation to expand dataset size to perform depression detection, which adds complexity to the training process. Moreover, integrating new modalities into LLMs compromises their inherent performance [38], [39], underscoring the need for optimized approaches in multimodal depression detection.

B. Information Entanglement Hypothesis

Based on our analysis of pre-trained models' limitations, we formulate a specific hypothesis about their poor performance in depression detection. Prior work has shown that both content and speech features contain depression-relevant information [40]. However, we hypothesize that the simultaneous encoding of these features within SSL model

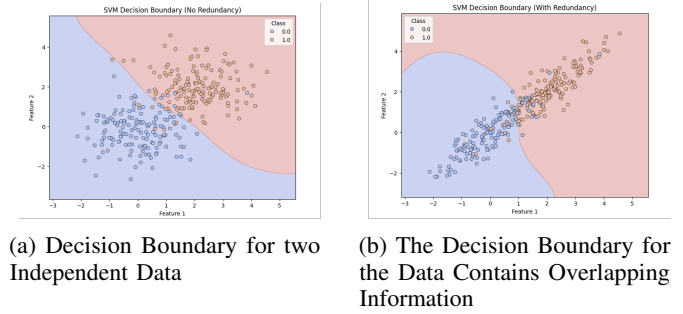


Fig. 4: A comparison of decision boundary for dependent/independent Data

representations impairs the model's ability to learn effective decision boundaries for depression detection.

To validate this hypothesis, we first demonstrate the impact of feature entanglement through controlled experiments with simulated data. Figure 4 presents two scenarios of binary classification: one with independent features (Figure 4a) and another with entangled features (Figure 4b). When features are independent, the classifier establishes a clear, linear decision boundary. In contrast, entangled features lead to a complex, non-linear decision boundary with regions of high uncertainty. This simulated demonstration aligns with our hypothesis that feature entanglement in SSL models creates similar classification challenges in depression detection.

To empirically test this hypothesis, we develop an information separation framework that explicitly disentangles content and speech features within SSL representations. If our hypothesis holds, this separation should lead to improved classification performance compared to standard SSL approaches that allow feature entanglement.

V. INFORMATION SEPARATION FRAMEWORK FOR DEPRESSION DETECTION

Figure 5 introduces our proposed framework for addressing the limitations of pre-trained models in depression detection. Motivated by our hypothesis about feature entanglement, we design an information separation module (left side) that explicitly disentangles modality-specific features into dense vectors. On the right side, we demonstrate how these separated features can be effectively integrated with frozen LLM embeddings for depression detection.

Through this framework, we investigate three research questions that directly address the limitations identified in pre-trained models:

RQ1: Can explicit separation of speech-specific and content-specific features improve depression detection performance? This question tests our core hypothesis about feature entanglement.

RQ2: How does utilizing information across multiple SSL model layers impact depression detection performance? This explores whether the limitation stems from single-layer feature extraction.

RQ3: Can frozen LLM embeddings with appropriate prompting achieve better performance than fine-tuning approaches?

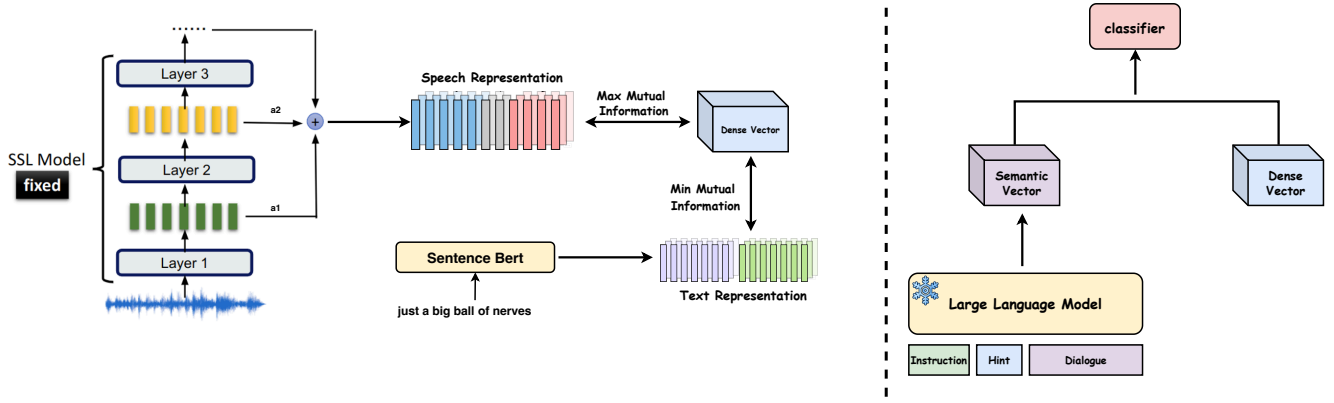


Fig. 5: Overview of the proposed information separation system for depression detection. On the left, the system separates information, constructing dense vectors that contain only speech-specific information. On the right, these dense vectors are integrated with an LLM for performing depression detection.

Here we examine whether fine-tuning might actually impair the model’s ability to leverage its pre-trained knowledge.

Each research question motivates a series of experiments in our subsequent analysis, designed to systematically evaluate our proposed solution against the limitations of current approaches.

A. Design of the Information Separation System

Building on our hypothesis about feature entanglement, we first design and evaluate systems for explicit information separation. We develop two parallel approaches: one that isolates speech-specific information and another that preserves only text-specific information. This design allows us to systematically test whether separated features outperform entangled representations in depression detection.

To achieve this separation, we implement a contrastive learning framework [41] that explicitly disentangles modality-specific information from the mixed representations in SSL models. The framework uses contrastive objectives to maximize the preservation of one modality’s information while minimizing interference from the other, resulting in specialized dense vectors for each modality. This approach directly tests our hypothesis about the detrimental effects of feature entanglement in pre-trained models.

The process begins by aggregating information distributed across the layers of a speech SSL model. Let $\mathbf{H} = \{h_1, h_2, \dots, h_L\}$ represent the hidden states from L layers for a given input. We compute a weighted sum [42] of these hidden states to form a compact representation:

$$h_{\text{speech}}^{(i)} = \sum_{l=1}^L \alpha_i^{(l)} h_l^{(i)} \quad (3)$$

where $h_l^{(i)}$ is the hidden state of the l -th layer for sample i , and $\alpha_i^{(l)}$ are learnable weights normalized such that $\sum_{l=1}^L \alpha_i^{(l)} = 1$. This weighted sum captures relevant information across layers for downstream tasks.

Next, we project the aggregated speech features $h_{\text{speech}}^{(i)}$ and the corresponding sentence-level features $s^{(i)}$ into a shared latent space using dense networks:

$$z_{\text{speech}}^{(i)} = \text{LeakyReLU}(\mathbf{W}_{\text{speech}} h_{\text{speech}}^{(i)} + \mathbf{b}_{\text{speech}}) \quad (4)$$

$$z_{\text{sentence}}^{(i)} = \text{LeakyReLU}(\mathbf{W}_{\text{sentence}} s^{(i)} + \mathbf{b}_{\text{sentence}}) \quad (5)$$

where $\mathbf{W}_{\text{speech}}$ and $\mathbf{W}_{\text{sentence}}$ are learnable weight matrices, and $\mathbf{b}_{\text{speech}}$ and $\mathbf{b}_{\text{sentence}}$ are biases. These projections ensure that both modalities are represented in a comparable space.

The dense vector $\mathbf{v} \in \mathbb{R}^d$ is trained to retain speech-specific information. This is achieved by maximizing the information between \mathbf{v} and z_{speech} while minimizing its information with z_{sentence} . Information is measured using cosine similarity:

$$\text{sim}_{\text{speech}} = \frac{\mathbf{v} \cdot z_{\text{speech}}}{\|\mathbf{v}\| \|z_{\text{speech}}\|} \quad (6)$$

$$\text{sim}_{\text{sentence}} = \frac{\mathbf{v} \cdot z_{\text{sentence}}}{\|\mathbf{v}\| \|z_{\text{sentence}}\|} \quad (7)$$

To achieve this objective, we employ a contrastive loss function:

$$\mathcal{L}_{\text{Loss}} = -\frac{1}{N} \sum_{i=1}^N \log \frac{\exp(\text{sim}_{\text{speech}}^{(i)}/\tau)}{\exp(\text{sim}_{\text{speech}}^{(i)}/\tau) + \exp(\text{sim}_{\text{sentence}}^{(i)}/\tau)} \quad (8)$$

where τ is a temperature parameter that controls the sharpness of the similarity distribution. This loss ensures that the dense vector aligns closely with the speech features while diverging from text-derived information, effectively filtering out content not unique to speech.

By optimizing this loss, the dense vector \mathbf{v} learns to isolate speech-specific information. Parameters updated during training include the dense network weights ($\mathbf{W}_{\text{speech}}$, $\mathbf{W}_{\text{sentence}}$), the dense vector \mathbf{v} , and the layer weights $\alpha_i^{(l)}$.

When the goal is to enable the dense vector to capture only content-related information, we adjust the contrastive loss function accordingly. Instead of emphasizing the separation of speech-specific information, the modified loss function promotes similarity between the dense vector and sentence embeddings while minimizing its similarity with speech embeddings. The reformulated contrastive loss is defined as follows:

$$\mathcal{L}_{\text{Loss}} = -\frac{1}{N} \sum_{i=1}^N \log \frac{\exp(\text{sim}_{\text{sentence}}^{(i)}/\tau)}{\exp(\text{sim}_{\text{sentence}}^{(i)}/\tau) + \exp(\text{sim}_{\text{speech}}^{(i)}/\tau)} \quad (9)$$

where $\text{sim}_{\text{sentence}}^{(i)}$ and $\text{sim}_{\text{speech}}^{(i)}$ represent the cosine similarity of the dense vector with the sentence and speech projections,

respectively, for the i -th sample. By focusing on sentence similarity, this loss function encourages the dense vector to align more closely with content-related information.

To validate the effectiveness of multi-layer SSL features in depression detection and respond to research question two, we designed an experiment that solely maximizes the similarity between the dense vector and the weighted sum of SSL features. The reformulated loss is defined as follows:

$$\mathcal{L}_{\text{loss}} = -\frac{\mathbf{v} \cdot \mathbf{z}_{\text{speech}}}{\|\mathbf{v}\| \|\mathbf{z}_{\text{speech}}\|} \quad (10)$$

B. Integration of Separated Features with LLMs

The second component of our framework addresses how to effectively combine separated features with LLM capabilities (right side of Figure 5). Rather than fine-tuning the LLM, we keep it frozen and use explicit task-specific prompts (“hints”) to guide the extraction of relevant semantic embeddings. This design choice stems from our observation that fine-tuning might disrupt the model’s pre-trained knowledge. For example, we use prompts like:

“Extract the semantic embedding from the following dialogue for depression detection.”

This multimodal framework combines the acoustic features extracted from speech SSL models with semantic information derived from LLMs, providing a comprehensive representation for depression detection. The speech dense vectors, denoted as $\mathbf{v}_{\text{speech}}$, are constructed by aggregating sentence-level dense vectors generated by the SSL model. Specifically, the dense vector for each sample is computed by taking the mean of all sentence-level dense vectors:

$$\mathbf{v}_{\text{speech}} = \frac{1}{N} \sum_{i=1}^N \mathbf{v}_{\text{speech}}^{(i)}, \quad (11)$$

where $\mathbf{v}_{\text{speech}}^{(i)}$ represents the dense vector for the i -th sentence, and N is the total number of sentences in the dialogue. This aggregation captures both global and local acoustic information, which is crucial for identifying depression-related patterns.

Semantic embeddings were extracted using a pre-trained LLM such as LLaMA. To ensure the embeddings were task-specific, the LLM processes each dialogue using the tailored hint described above. The dialogue was encoded, and the hidden states of the final layer were mean-pooled to generate a fixed-size semantic embedding:

$$\mathbf{E}_{\text{LLM}} = \frac{1}{T} \sum_{t=1}^T \mathbf{h}_{\text{LLM}}^{(t)}, \quad (12)$$

where $\mathbf{h}_{\text{LLM}}^{(t)}$ denotes the hidden state at time step t , and T represents the sequence length. This embedding captures the semantic content of the dialogue in alignment with the depression detection task.

To improve computational efficiency and reduce redundancy in the high-dimensional LLM embeddings, we applied dimensionality reduction using UMAP [43]:

$$\mathbf{E}_{\text{LLM, reduced}} = \text{UMAP}(\mathbf{E}_{\text{LLM}}), \quad (13)$$

where we reduce the embedding dimension to 300 based on preliminary experiments that showed this preserves task-relevant information while reducing computational overhead.

The final multimodal representation combines the speech dense vector $\mathbf{v}_{\text{speech}}$ and the reduced LLM embedding $\mathbf{E}_{\text{LLM, reduced}}$:

$$\mathbf{F} = [\mathbf{v}_{\text{speech}}; \mathbf{E}_{\text{LLM, reduced}}], \quad (14)$$

where $[\cdot; \cdot]$ denotes concatenation. This integration creates a unified feature vector that preserves the separated modality-specific information while allowing their complementary use.

For classification, we deliberately choose a simple SVM classifier to ensure that any performance improvements can be attributed to our feature separation approach rather than classifier complexity. This allows us to directly evaluate how the quality of separated features impacts depression detection performance. To validate our framework’s effectiveness, we conduct experiments using both combined (\mathbf{F}) and independent modality features ($\mathbf{v}_{\text{speech}}$ and $\mathbf{E}_{\text{LLM, reduced}}$), focusing on how feature separation affects model performance.

VI. EVALUATING THE INFORMATION SEPARATION HYPOTHESIS

A. Experimental Setup for Information Separation

To systematically evaluate our hypothesis about feature entanglement, we conduct experiments across three scenarios using major SSL models (HuBERT [26], Wav2Vec2 [2], and WavLM [3]):

1. Speech-specific information preservation
2. Text-specific information preservation
3. Layer-wise information combination through learnable weights (ranging from 0 to 1, summing to 1 across layers)

Implementation details: batch size 64, 1500 epochs, temperature 0.1, learning rate 0.0001, Adam optimizer on V100 GPUs. Dense vector dimensions varied from 100 to 500 to study dimensionality impact.

B. Validating the Benefits of Information Separation

Our experiments with SSL models demonstrate the impact of information separation through two key findings. First, combining information across layers yields model-specific benefits - substantial improvements for Wav2Vec and HuBERT but minimal gains for WavLM (Tables IV, III). This suggests that the distribution of depression-relevant information varies across model architectures. More importantly, explicit separation of speech-specific and text-specific information consistently improves performance in all approaches. The speech-specific system particularly excels, outperforming even data-augmented baselines (Table II) and achieving state-of-the-art results for SSL models in depression detection. This superior performance without data augmentation validates our core hypothesis: feature entanglement, rather than model capacity, has been the key factor limiting SSL model performance in depression detection.

TABLE IV: F1 Scores Across Dense Vector Dimensions for Different Objectives and Speech SSL Models. ‘‘Speech Information Preservation’’ denotes Dense Vectors containing only speech-related information, ‘‘Text Information Preservation’’ focuses on text-related information, and ‘‘Weighted Sum Similarity Maximization’’ maximizes similarity between Dense Vectors and weighted Speech SSL features.

Dimension	WavLM			Wav2Vec			HuBERT		
	F1-avg	F1-max	F1-std	F1-avg	F1-max	F1-std	F1-avg	F1-max	F1-std
Speech Information Preservation									
100	0.552	0.571	0.014	0.540	0.546	0.012	0.549	0.558	0.006
200	0.618	0.621	0.003	0.512	0.514	0.002	0.591	0.621	0.020
300	0.755	0.769	0.016	0.525	0.533	0.010	0.600	0.615	0.017
400	0.563	0.585	0.015	0.586	0.615	0.035	0.534	0.537	0.002
500	0.634	0.640	0.012	0.616	0.640	0.030	0.676	0.688	0.022
Text Information Preservation									
100	0.521	0.522	0.000	0.526	0.529	0.004	0.602	0.625	0.022
200	0.554	0.564	0.007	0.602	0.611	0.012	0.558	0.558	0.000
300	0.641	0.667	0.030	0.528	0.546	0.012	0.580	0.606	0.017
400	0.608	0.615	0.015	0.616	0.621	0.010	0.530	0.533	0.006
500	0.595	0.600	0.011	0.571	0.571	0.000	0.656	0.667	0.012
SSL Weighted Sum Similarity Maximization									
100	0.563	0.585	0.017	0.601	0.625	0.019	0.552	0.556	0.008
200	0.638	0.667	0.058	0.537	0.546	0.011	0.628	0.643	0.028
300	0.519	0.522	0.006	0.550	0.564	0.020	0.522	0.522	0.000
400	0.574	0.621	0.033	0.612	0.615	0.008	0.548	0.556	0.015
500	0.557	0.571	0.010	0.619	0.632	0.008	0.627	0.643	0.031

C. Quantifying Information Separation in Dense Vectors

Building on our hypothesis that feature entanglement impairs model performance, we analyze what makes our separation approach effective. A key question emerges from the results in Figure 6a: why do different models require different dense vector dimensions for optimal performance (300 for WavLM, 500 for HuBERT)? We propose that the effectiveness of separation depends on finding the right balance between representational capacity and information disentanglement. To verify this, we measure the degree of separation using Mutual Information Neural Estimation (MINE) [44]:

$$I_{\Theta}(\mathbf{v}, \mathbf{e}) = \sup_{\theta \in \Theta} \mathbb{E}_{P(\mathbf{v}, \mathbf{e})} [T_{\theta}(\mathbf{v}, \mathbf{e})] - \log \mathbb{E}_{P(\mathbf{v})P(\mathbf{e})} [e^{T_{\theta}(\mathbf{v}, \mathbf{e})}], \quad (15)$$

where T_{θ} is a trainable neural network parameterized by θ , $P(\mathbf{v}, \mathbf{e})$ represents the joint distribution, and $P(\mathbf{v})P(\mathbf{e})$ is the product of the marginal distributions. Our analysis reveals that performance peaks when mutual information reaches its minimum (Figure 6b), indicating that better separation directly leads to better depression detection. However, achieving this separation requires sufficient dimensionality - too few dimensions (as seen at 100) constrain the model’s ability to properly separate features while preserving task-relevant information [44], [45]. This explains why optimal dimensions vary across models: each architecture requires different representational capacity to achieve effective separation.

D. Layer-Level Analysis of Information in Dense Vector

Building on the insights from the information separation analysis in the previous section, we delve deeper into how layer-

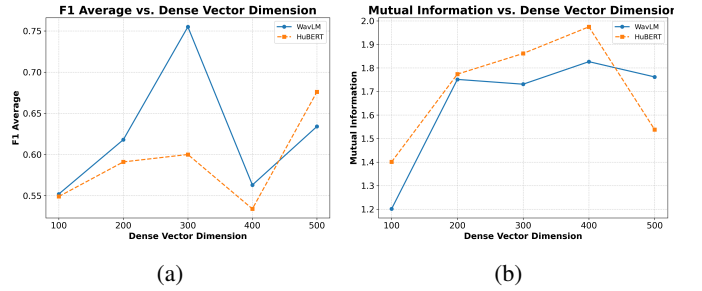


Fig. 6: A comparison of mutual information and performance in Speech Dense Vector for WavLM and HuBERT

wise representations contribute to this separation process. Since WavLM consistently achieves the best performance across all speech SSL models, our analysis primarily focuses on WavLM. Figure 7a reveals that layer weights for extracting speech-specific information via contrastive learning are predominantly concentrated in the deeper layers, which are known to encode high-level semantic and emotional information [3] encompassing both content-related and speech-specific features. By leveraging Sentence-BERT embeddings, the contrastive learning framework disentangles these features, isolating speech-specific information while filtering out content-related aspects, reducing the overlap between the two and validating our earlier hypothesis.

Interestingly, Figure 7b demonstrates a different pattern for extracting text-specific information, with weights distributed across both earlier and deeper layers, peaking around Layer 2 and Layer 10. This pattern suggests that text-specific information leverages features across a broader range of layers, reflecting its inherently mixed nature within speech SSL models. The consistency of these trends across dense vector dimensions underscores the robustness of these observations and highlights the targeted nature of contrastive learning in shaping layer-wise representations to align with specific objectives.

The layer weight distributions for HuBERT and Wav2Vec2, as shown in Figure 7c and Figure 7d, reveal the impact of pre-training methodologies on the representation of speech-specific information. HuBERT’s distribution closely resembles WavLM’s, with weights concentrated in the deeper layers, peaking around layers 10 to 12. By contrast, Wav2Vec2 displays a more distributed pattern, with less reliance on deeper layers. This contrast highlights the role of training strategies in shaping information distribution. HuBERT and WavLM share similar masked prediction tasks on discretized pseudo-labels during pre-training, which likely drives their deeper layers to encode nuanced speech-specific features. Meanwhile, Wav2Vec2’s contrastive learning approach results in a different allocation of information across layers. These findings suggest that pre-training methodology fundamentally influences how speech and content information are organized within the model, shaping its suitability for downstream tasks like depression detection.

E. How the Model Detects Depression by Dense Vector?

Understanding how a depression detection system makes decisions is essential, as it ensures transparency and fosters trust in its outcomes. In our baseline framework, we introduced

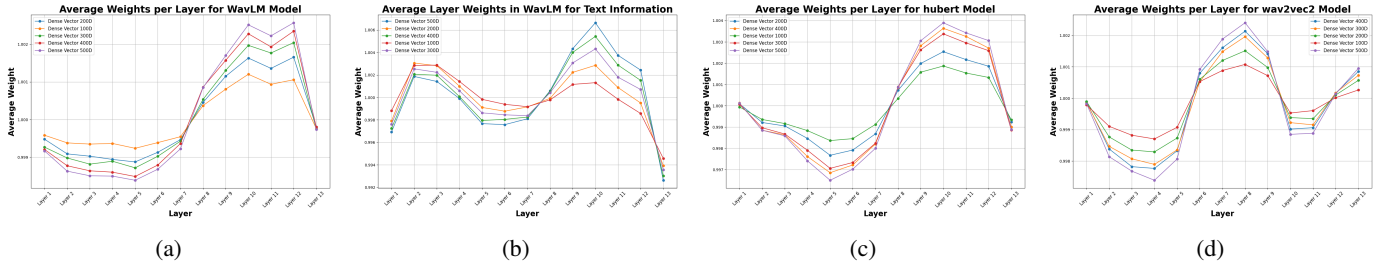


Fig. 7: Average Weight of Different Speech SSL Models When Learning Dense Vector

a depression detection system grounded in acoustic landmarks, with each landmark offering linguistically interpretable insights. Building on this approach, we extended the system to extract temporal information from speech using acoustic landmarks, aiming to enhance the interpretability of the dense vector depression detection system.

Our approach analyzes the most influential sentences in each file based on their impact on classification decisions. We select five sentences per file, following established practices in interpretable machine learning that suggest a small subset of high-impact examples provides better interpretability than analyzing all instances [46], [47]. This focused analysis allows us to identify clear patterns in how our model makes decisions while maintaining tractable computational complexity. The five-sentence threshold balances between capturing sufficient variation in speech patterns and maintaining clear interpretability of results.

Identifying Key Sentences. To identify the most important sentences in a document for depression detection, we analyze how the removal of each sentence affects the SVM classifier’s decision value. Given a document-level dense vector \mathbf{v}_{doc} , represented as the average of sentence-level dense vectors $\{\mathbf{v}_1, \mathbf{v}_2, \dots, \mathbf{v}_n\}$:

$$\mathbf{v}_{\text{doc}} = \frac{1}{n} \sum_{i=1}^n \mathbf{v}_i, \quad (16)$$

the decision value for the SVM classifier is computed as:

$$D_{\text{original}} = f(\mathbf{v}_{\text{doc}}), \quad (17)$$

where $f(\cdot)$ is the decision function of the SVM.

For each sentence \mathbf{v}_i , we construct a modified document-level vector $\mathbf{v}_{\text{modified}}$ by excluding the i -th sentence:

$$\mathbf{v}_{\text{modified}} = \frac{1}{n-1} \sum_{j \neq i} \mathbf{v}_j. \quad (18)$$

The modified decision value is calculated as:

$$D_{\text{modified},i} = f(\mathbf{v}_{\text{modified}}). \quad (19)$$

The importance of the i -th sentence is quantified as the absolute change in the decision value:

$$\Delta D_i = |D_{\text{original}} - D_{\text{modified},i}|. \quad (20)$$

The sentences are ranked based on their ΔD_i values, with the top five sentences selected as the most influential for the model’s prediction. For each document, this procedure also provides insight into which sentences most significantly contribute to the classification decision.

Landmark Bigram Duration Analysis After identifying the most influential sentences, we aim to explore their common characteristics and uncover the distinguishing features that the machine learning model leverages to differentiate between healthy individuals and those with depression. Previous research has demonstrated significant differences in temporal characteristics [33], [18], such as speaking rate and pauses, between individuals with depression and healthy individuals. The acoustic landmarks in our baseline system provide a promising approach for analyzing the temporal structure of speech signals. More precisely, we derived several statistical features from the time durations between consecutive acoustic landmarks.

Each important sentence was annotated with a sequence of landmarks. For each landmark l_i , its timestamp was denoted by $t(l_i)$. The duration between two adjacent landmarks l_i and l_{i+1} was defined as:

$$d_{i \rightarrow i+1} = t(l_{i+1}) - t(l_i), \quad (21)$$

where $i \in \{1, \dots, n-1\}$ and n is the total number of landmarks in a given sentence.

To quantify the temporal characteristics of speech in depressed and healthy individuals, we calculated statistical features for the duration of each landmark bigram. For a given landmark bigram [18], [48] $b_{n \rightarrow m}$, where $n, m \in \{g, p, s, f, v, b\}$ its durations are aggregated across all samples, forming a set $D_{b_{n \rightarrow m}} = \{d_{n \rightarrow m}^1, d_{n \rightarrow m}^2, \dots, d_{n \rightarrow m}^y\}$. The k -th statistical feature for this set was computed as:

$$d_k = |D_{b_{n \rightarrow m}}|_k, \quad (22)$$

where $|\cdot|_k$ represents a specific statistical measure.

We calculated a series of features, including mean, median, variance, standard deviation, minimum, maximum interquartile range, skewness and kurtosis, to summarize the temporal dynamics of each bigram. These features collectively describe the differences in timing patterns between healthy and depressed individuals.

To evaluate the statistical significance of these differences, we conducted a Mann-Whitney U test for each bigram $b_{n \rightarrow m}$ to compare the duration distributions between the two groups. The test produces a U-statistic and a p-value, indicating whether the differences are statistically significant. Bigram pairs with p-values below the threshold of 0.05 are identified as having significant differences, highlighting the landmark transitions most relevant to distinguishing depressed and healthy individuals.

Results and Interpretation Our analysis identified two landmark bigrams b_{-g+} and p_{+b-} as exhibiting the most

significant differences in duration distributions between healthy and depressed individuals when compared with other landmark pairs. From a statistical perspective, these findings confirm that there are observable differences in speech timing characteristics between healthy individuals and those with depression. These distinctions in landmark duration patterns provide evidence that speech timing information carries meaningful variations between the two groups, aligning with the model’s ability to leverage such acoustic features for classification.

The $b-g+$ bigram captures the transition from the cessation of turbulent noise ($b-$) to the onset of vocal fold vibration ($g+$). This transition often corresponds to the release of a voiced obstruent, a feature influenced by both articulation precision and timing [49]. Similarly, the $p+-b-$ bigram represents the shift from the onset of periodicity ($p+$)—indicative of voiced sound initiation—to the offset of turbulent noise ($b-$), which is associated with the termination of an obstruent region [49].

The prominence of these landmark pairs highlights that depression may affect the fine-grained timing and coordination of speech production mechanisms, particularly in transitions involving voicing and turbulence. Such temporal shifts could be related to changes in motor control, vocal fold tension, or articulatory effort, which have been observed in prior studies on speech characteristics of individuals with depression [50], [51]. These findings reinforce the importance of leveraging temporal acoustic features for uncovering depression-specific speech patterns.

VII. LARGE LANGUAGE MODEL RESULTS AND ANALYSIS

A. LLM Experiment Setup

To ensure a comprehensive comparison with previous work, we conducted experiments on four models: Llama2-7B, Llama2-7B Chat, Llama2-13B, and Llama2-13B Chat. All models were frozen to extract embeddings without fine-tuning. The experiments were performed on an NVIDIA A100 GPU with 80GB of memory. The downstream classification model used is consistent with the SVM setup described earlier.

B. LLM Experiment Results

Table V summarizes the F1 scores across various Llama2-based models with different embedding dimensions and the inclusion or exclusion of depression-related information (denoted as "Dep. Info").

From the results, we observe that models incorporating depression information consistently outperform their counterparts without it. For example, the Llama2 7B Chat model achieves a notable increase in F1-avg from 0.5259 (without depression information) to 0.6812 (with depression information) at the 300-dimensional setting, with a similar trend observed for other dimensions. This highlights the importance of including depression-specific information in embeddings to improve classification performance.

Among the models, Llama2 7B exhibited high consistency in their F1 scores. The Llama2 7B model achieves identical F1-avg and F1-max values of 0.6667 across all configurations, regardless of embedding dimensions or the inclusion of depression-related information, with F1-std values

TABLE V: F1 Scores Across Different Large Language Models, Embedding Dimensions. Dep Info indicates if contains a hint of depression information.

Model	Dim.	Dep. Info	F1-avg	F1-max	F1-std
Llama2 7B Chat	300	✗	0.5259	0.5366	0.0072
	300	✓	0.6812	0.6957	0.0167
	500	✗	0.6191	0.6667	0.0550
	500	✓	0.6202	0.6364	0.0325
Llama2 7B	300	✗	0.6667	0.6667	0.0000
	300	✓	0.6667	0.6667	0.0000
	500	✗	0.6618	0.6667	0.0098
	500	✓	0.6667	0.6667	0.0000
Llama2 13B Chat	300	✗	0.629	0.6667	0.0429
	300	✓	0.667	0.6667	0.0000
	500	✗	0.6300	0.6400	0.0200
	500	✓	0.6600	0.6667	0.0134
Llama2 13B	300	✗	0.5976	0.6286	0.0449
	300	✓	0.6270	0.6667	0.0282
	500	✗	0.5786	0.6000	0.0143
	500	✓	0.6559	0.6667	0.0124
Previous SOTA [4]	-	-	0.756	0.800	0.023
Chat 7B + Wavlm	300	✓	0.76655	0.7692	0.0053

consistently near zero. This phenomenon indicates that the embeddings of Llama2 7B lack diversity, which might be attributed to the absence of reinforcement learning from human feedback (RLHF). In contrast, the Llama2 7B Chat model also demonstrates strong performance, but its F1-avg values exhibit greater variability across configurations, such as 0.5259 for 300 dimensions without depression information compared to 0.6812 with depression information. This variability underscores the influence of RLHF in enhancing the output diversity of the model.

When comparing models of different scales, the Llama2 13B models do not consistently outperform their smaller counterparts (Llama2 7B). For instance, at the 500-dimensional setting with depression information, the Llama2 13B model achieves an F1-avg of 0.6559, slightly lower than the 0.6667 achieved by the Llama2 7B. Additionally, the Llama2 13B Chat model achieves an F1-avg of 0.6600 in this setting, still slightly behind the Llama2 7B. These findings indicate that increased model capacity does not always translate into superior performance.

Additionally, combining the best-performing models from each modality—Llama2 7B Chat for text-based features and WavLM for speech-based dense vectors yields the highest overall performance. This integration achieves an average F1 of 0.7665 and a max F1 of 0.769 at the 300-dimensional setting, surpassing previous state-of-the-art results that relied on WavLM Layer 10 and Roberta with extensive data augmentation. Notably, our approach achieves this performance without leveraging any form of data augmentation, demonstrating the robustness and effectiveness of combining complementary features from specialized text and speech models.

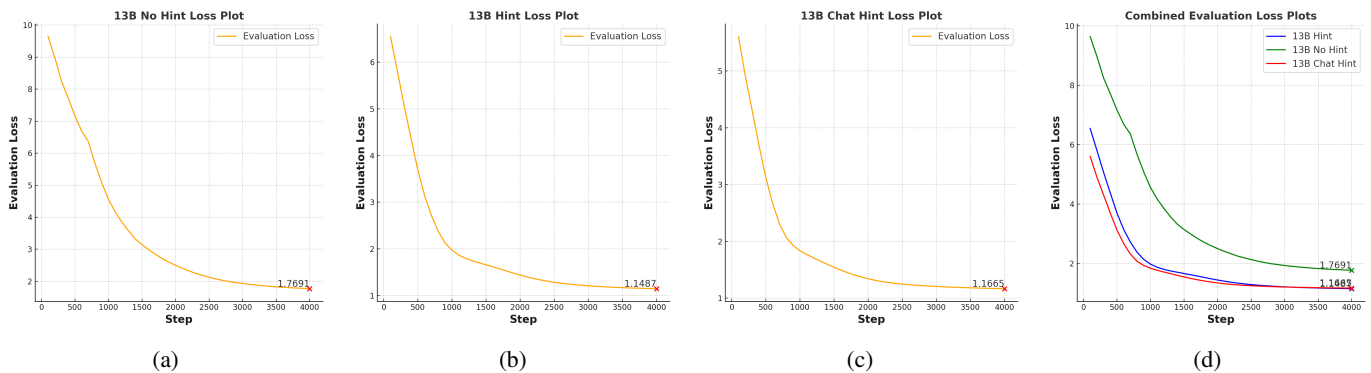


Fig. 8: Evaluation Loss for Different Configurations up to 4000 Steps for Baseline Cross-model Instruction Tuning.

C. The Critical Role of Hints in Baseline and Advanced Systems

The inclusion of hints—providing information about whether a data sample originates from a depressed or healthy individual—has demonstrated significant value across both the baseline system and the new LLM-based systems. While the mechanisms differ between the two setups, the impact of embedding task-specific information remains evident in both.

In the baseline system, hints are directly integrated into the Cross-modal Instruction Training process, and their influence is clearly illustrated by the evaluation loss trends shown in Figure 8. When no hint was provided, the loss converged to a higher value of approximately 1.76 (Figure 8a). By contrast, the presence of hints led to a significant improvement, with the loss consistently converging to around 1.1 (Figures 8b and 8c). Figure 8d further emphasizes this disparity, demonstrating the role of hints in driving better convergence behavior. These results highlight that embedding depression-related information enhances the model’s ability to differentiate between healthy and depressed speech patterns.

In the new system, which utilizes pre-trained and frozen LLM embeddings, hints are not used during LLM training but are incorporated into downstream processing to augment task-specific contextual information. Table V clearly reflects the benefit of hints across different LLM configurations. For example, in the Llama2 7B Chat model with 300-dimensional embeddings, the F1-avg improved from 0.5259 without hints to 0.6812 with hints. A similar pattern was observed across other models, such as Llama2 13B, where the F1-avg increased from 0.5786 to 0.6559 with the inclusion of depression-related information. These improvements demonstrate that even without modifying the LLMs themselves, incorporating hints into the downstream analysis substantially enhances performance.

The consistent findings across both the baseline and our advanced LLM-based systems underscore the critical role of providing explicit task-related information, such as hints, during depression detection. In the baseline system, hints enable the model to focus on relevant speech features, such as temporal and acoustic patterns, that distinguish healthy individuals from those with depression. Similarly, in the advanced LLM-based system, hints serve as explicit task signals, guiding the embeddings toward more relevant semantic

TABLE VI: Quantitative Metrics for 7B and 7B Chat Embeddings

LlaMA2	Hint	Cosine Mean	Pairwise Dist.	Var./Dim.
7B	✗	0.9500	18.65	0.0457
	✓	0.9503	18.57	0.0463
7B Chat	✗	0.9374	20.01	0.0536
	✓	0.9373	19.93	0.0533

spaces that align with depression classification. By clearly defining the task context, hints help LLMs prioritize task-relevant distinctions, demonstrating that even without fine-tuning, embedding task-specific information into pre-trained models significantly enhances their utility for specialized tasks like depression detection.

D. LLM Embedding Diversity Analysis

To understand why frozen LLM embeddings outperform fine-tuned approaches, we analyze the embedding properties of Llama2 7B and 7B Chat models. Our analysis focuses on three key metrics that characterize embedding quality and diversity: cosine similarity, pairwise distance, and variance per dimension (Table VI). Cosine similarity measures the alignment between embeddings by calculating the average angle between all pairs in the high-dimensional space. Higher similarity values indicate a more homogeneous embedding representation. Pairwise distance, computed as the mean Euclidean distance across embedding pairs, quantifies the degree of clustering in the embedding space, with lower values reflecting tighter clustering. Variance per dimension captures the distribution of information across the embedding space, with higher variance suggesting a more diverse and expressive representation. These metrics collectively provide a detailed understanding of the structural differences between embeddings generated by the two models.

When comparing the Chat and non-Chat versions, the embeddings generated by the Llama2 7B Chat model exhibit lower cosine similarity values, with embeddings showing less alignment compared with the Llama2 7B model. Specifically, the cosine similarity for the Llama2 7B Chat model reflects

a broader diversity in embedding representations. Pairwise distances between embeddings are also larger for the Llama2 7B Chat model, indicating that its embeddings occupy a wider feature space. Additionally, the variance per dimension for the Llama2 7B Chat model is consistently higher across both configurations, reflecting a richer and more distributed representation compared to the Llama2 7B model, which shows lower variance. This observation also explains the minimal variation in F1 scores observed for the Llama2 7B model in Table V. The tightly clustered embeddings and lower variance per dimension suggest that the Llama2 7B model captures less diverse information, resulting in consistent but less adaptive performance across different configurations. In contrast, the broader representation space of the Llama2 7B Chat model enables it to better adapt to nuanced task requirements, which is reflected in its sensitivity to the inclusion of depression-related hints.

We also observed that introducing hints led to a decrease in embedding diversity across all metrics in Table VI. This reduction in diversity is reflected in Table V, where the inclusion of hints consistently lowers the F1-std for the same model with the same embedding dimension. This suggests that providing task-specific information helps the model generate more consistent embeddings, resulting in reduced variability in classification performance.

VIII. CONCLUSION

In this study, we investigated why pre-trained models struggle with multi-modal depression detection and proposed a solution through information separation. Our investigation revealed that the poor performance of these models stems from the entanglement of content and speech-specific features, rather than limitations in model capacity. By systematically testing this hypothesis, we demonstrated that explicit separation of speech and content information significantly improves performance without requiring data augmentation. For SSL models, our information separation framework achieved state-of-the-art results by disentangling modality-specific features, while for LLMs, we found that frozen embeddings with appropriate prompting outperform fine-tuning approaches, suggesting that preserving pre-trained knowledge while guiding feature extraction is crucial. Our findings contribute both theoretical understanding and practical solutions to multi-modal depression detection, demonstrating that careful consideration of how information is represented and processed is essential for effective depression detection systems.

ACKNOWLEDGEMENT

This work was supported by the Australian Research Council Discovery Project DP230101184.

REFERENCES

- [1] J. Walker, K. Burke, M. Wanat, R. Fisher, J. Fielding, A. Mulick, S. Puntis, J. Sharpe, M. Degli Esposti, E. Harriss, *et al.*, “The prevalence of depression in general hospital inpatients: a systematic review and meta-analysis of interview-based studies,” *Psychological medicine*, vol. 48, no. 14, pp. 2285–2298, 2018.
- [2] A. Baevski, Y. Zhou, A. Mohamed, and M. Auli, “wav2vec 2.0: A framework for self-supervised learning of speech representations,” *Advances in neural information processing systems*, vol. 33, pp. 12 449–12 460, 2020.
- [3] S. Chen, C. Wang, Z. Chen, Y. Wu, S. Liu, Z. Chen, J. Li, N. Kanda, T. Yoshioka, X. Xiao, *et al.*, “Wavlm: Large-scale self-supervised pre-training for full stack speech processing,” *IEEE Journal of Selected Topics in Signal Processing*, vol. 16, no. 6, pp. 1505–1518, 2022.
- [4] W. Wu, C. Zhang, and P. C. Woodland, “Self-supervised representations in speech-based depression detection,” in *ICASSP 2023-2023 IEEE International Conference on Acoustics, Speech and Signal Processing (ICASSP)*. IEEE, 2023, pp. 1–5.
- [5] Z. Bao, K. Qian, Z. Zhao, M. Sun, R. Huang, D. Xu, B. Hu, Y. Yamamoto, and B. W. Schuller, “Somatisation disorder detection via speech: Introducing a self-supervised learning model,” in *2023 45th Annual International Conference of the IEEE Engineering in Medicine & Biology Society (EMBC)*. IEEE, 2023, pp. 1–4.
- [6] A. Chowdhery, S. Narang, J. Devlin, M. Bosma, G. Mishra, A. Roberts, P. Barham, H. W. Chung, C. Sutton, S. Gehrmann, *et al.*, “Palm: Scaling language modeling with pathways,” *Journal of Machine Learning Research*, vol. 24, no. 240, pp. 1–113, 2023.
- [7] H. Touvron, L. Martin, K. Stone, P. Albert, A. Almahairi, Y. Babaei, N. Bashlykov, S. Batra, P. Bhargava, S. Bhosale, *et al.*, “Llama 2: Open foundation and fine-tuned chat models,” *arXiv preprint arXiv:2307.09288*, 2023.
- [8] N. Oh, G.-S. Choi, and W. Y. Lee, “Chatgpt goes to the operating room: evaluating gpt-4 performance and its potential in surgical education and training in the era of large language models,” *Annals of Surgical Treatment and Research*, vol. 104, no. 5, p. 269, 2023.
- [9] Z. Wang, R. Li, B. Dong, J. Wang, X. Li, N. Liu, C. Mao, W. Zhang, L. Dong, J. Gao, *et al.*, “Can llms like gpt-4 outperform traditional ai tools in dementia diagnosis? maybe, but not today,” *arXiv preprint arXiv:2306.01499*, 2023.
- [10] A. Lahat, E. Shachar, B. Avidan, Z. Shatz, B. S. Glicksberg, and E. Klang, “Evaluating the use of large language model in identifying top research questions in gastroenterology,” *Scientific reports*, vol. 13, no. 1, p. 4164, 2023.
- [11] S. A. Liu, “Landmark detection for distinctive feature-based speech recognition,” *The Journal of the Acoustical Society of America*, vol. 100, no. 5, pp. 3417–3430, 1996.
- [12] X. Zhang, D. Liu, T. Xiao, C. Xiao, T. Szalay, M. Shahin, B. Ahmed, and J. Epps, “Auto-landmark: Acoustic landmark dataset and open-source toolkit for landmark extraction,” *arXiv preprint arXiv:2409.07969*, 2024.
- [13] K. N. Stevens, “Toward a model for lexical access based on acoustic landmarks and distinctive features,” *The Journal of the Acoustical Society of America*, vol. 111, no. 4, pp. 1872–1891, 2002.
- [14] X. Zhang, H. Liu, K. Xu, Q. Zhang, D. Liu, B. Ahmed, and J. Epps, “When LLMs meets acoustic landmarks: An efficient approach to integrate speech into large language models for depression detection,” in *Proceedings of the 2024 Conference on Empirical Methods in Natural Language Processing*, Y. Al-Onaizan, M. Bansal, and Y.-N. Chen, Eds. Miami, Florida, USA: Association for Computational Linguistics, Nov. 2024, pp. 146–158.
- [15] P. L. Garvin, “Preliminaries to speech analysis: The distinctive features and their correlates,” 1953.
- [16] D. He, X. Yang, B. P. Lim, Y. Liang, M. Hasegawa-Johnson, and D. Chen, “When etc training meets acoustic landmarks,” in *ICASSP 2019-2019 IEEE International Conference on Acoustics, Speech and Signal Processing (ICASSP)*. IEEE, 2019, pp. 5996–6000.
- [17] Z. Huang, J. Epps, D. Joachim, and M. Chen, “Depression detection from short utterances via diverse smartphones in natural environmental conditions,” in *INTERSPEECH*, 2018, pp. 3393–3397.
- [18] Z. Huang, J. Epps, and D. Joachim, “Investigation of speech landmark patterns for depression detection,” *IEEE transactions on affective computing*, vol. 13, no. 2, pp. 666–679, 2019.
- [19] S. Boyce, H. Fell, and J. MacAuslan, “Speechmark: Landmark detection tool for speech analysis,” in *Thirteenth Annual Conference of the International Speech Communication Association*, 2012.
- [20] W. S. Noble, “What is a support vector machine?” *Nature biotechnology*, vol. 24, no. 12, pp. 1565–1567, 2006.
- [21] N. Cummins, J. Epps, M. Breakspear, and R. Goecke, “An investigation of depressed speech detection: Features and normalization,” in *Twelfth Annual Conference of the International Speech Communication Association*, 2011.
- [22] A. Gulati, J. Qin, C.-C. Chiu, N. Parmar, Y. Zhang, J. Yu, W. Han, S. Wang, Z. Zhang, Y. Wu, *et al.*, “Conformer: Convolution-augmented

- transformer for speech recognition,” *arXiv preprint arXiv:2005.08100*, 2020.
- [23] X. Zhang, Q. Zhang, H. Liu, T. Xiao, X. Qian, B. Ahmed, E. Ambikairajah, H. Li, and J. Epps, “Mamba in speech: Towards an alternative to self-attention,” *arXiv preprint arXiv:2405.12609*, 2024.
- [24] Z. Zhao, Z. Bao, Z. Zhang, N. Cummins, H. Wang, and B. Schuller, “Hierarchical attention transfer networks for depression assessment from speech,” in *ICASSP 2020-2020 IEEE international conference on acoustics, speech and signal processing (ICASSP)*. IEEE, 2020, pp. 7159–7163.
- [25] Y. Shen, H. Yang, and L. Lin, “Automatic depression detection: An emotional audio-textual corpus and a gru/bilstm-based model,” in *ICASSP 2022-2022 IEEE International Conference on Acoustics, Speech and Signal Processing (ICASSP)*. IEEE, 2022, pp. 6247–6251.
- [26] W.-N. Hsu, B. Bolte, Y.-H. H. Tsai, K. Lakhota, R. Salakhutdinov, and A. Mohamed, “Hubert: Self-supervised speech representation learning by masked prediction of hidden units,” *IEEE/ACM Transactions on Audio, Speech, and Language Processing*, vol. 29, pp. 3451–3460, 2021.
- [27] H. Liu, L. P. G. Perera, A. W. H. Khong, E. S. Chng, S. J. Styles, and S. Khudanpur, “Efficient self-supervised learning representations for spoken language identification,” *IEEE J. Sel. Topics Signal Process.*, vol. 16, no. 6, pp. 1296–1307, 2022.
- [28] Y. Liu, M. Ott, N. Goyal, J. Du, M. Joshi, D. Chen, O. Levy, M. Lewis, L. Zettlemoyer, and V. Stoyanov, “Roberta: A robustly optimized bert pretraining approach,” *arXiv preprint arXiv:1907.11692*, 2019.
- [29] E. J. Hu, Yelong shen, P. Wallis, Z. Allen-Zhu, Y. Li, S. Wang, L. Wang, and W. Chen, “LoRA: Low-rank adaptation of large language models,” in *Proc. Int. Conf. Learn. Representations*, 2022.
- [30] X. L. Li and P. Liang, “Prefix-tuning: Optimizing continuous prompts for generation,” in *Proceedings of the 59th Annual Meeting of the Association for Computational Linguistics and the 11th International Joint Conference on Natural Language Processing (Volume 1: Long Papers)*, 2021, pp. 4582–4597.
- [31] X. Liu, Y. Zheng, Z. Du, M. Ding, Y. Qian, Z. Yang, and J. Tang, “Gpt understands, too,” *AI Open*, 2023. [Online]. Available: <https://www.sciencedirect.com/science/article/pii/S2666651023000141>
- [32] E. B. Zaken, Y. Goldberg, and S. Ravfogel, “Bitfit: Simple parameter-efficient fine-tuning for transformer-based masked language-models,” in *Proceedings of the 60th Annual Meeting of the Association for Computational Linguistics (Volume 2: Short Papers)*, 2022, pp. 1–9.
- [33] N. Cummins, S. Scherer, J. Krajewski, S. Schnieder, J. Epps, and T. F. Quatieri, “A review of depression and suicide risk assessment using speech analysis,” *Speech communication*, vol. 71, pp. 10–49, 2015.
- [34] D. DeVault, R. Artstein, G. Benn, T. Dey, E. Fast, A. Gainer, K. Georgila, J. Gratch, A. Hartholt, M. Lhommet, *et al.*, “Simsensei kiosk: A virtual human interviewer for healthcare decision support,” in *Proceedings of the 2014 international conference on Autonomous agents and multi-agent systems*, 2014, pp. 1061–1068.
- [35] Y. Gong and C. Poellabauer, “Topic modeling based multi-modal depression detection,” in *Proceedings of the 7th annual workshop on Audio/Visual emotion challenge*, 2017, pp. 69–76.
- [36] W. Wu, M. Wu, and K. Yu, “Climate and weather: Inspecting depression detection via emotion recognition,” in *ICASSP 2022-2022 IEEE International Conference on Acoustics, Speech and Signal Processing (ICASSP)*. IEEE, 2022, pp. 6262–6266.
- [37] J. Bergstra, R. Bardenet, Y. Bengio, and B. Kégl, “Algorithms for Hyper-Parameter Optimization,” in *Advances in Neural Information Processing Systems*, vol. 24. Curran Associates, Inc., 2011.
- [38] R. Zhang, J. Han, A. Zhou, X. Hu, S. Yan, P. Lu, H. Li, P. Gao, and Y. Qiao, “Llama-adapter: Efficient fine-tuning of language models with zero-init attention,” *arXiv preprint arXiv:2303.16199*, 2023.
- [39] Y. Li, Y. Wu, J. Li, and S. Liu, “Prompting large language models for zero-shot domain adaptation in speech recognition,” *arXiv preprint arXiv:2306.16007*, 2023.
- [40] W. Zheng, L. Yan, and F.-Y. Wang, “Two birds with one stone: Knowledge-embedded temporal convolutional transformer for depression detection and emotion recognition,” *IEEE Transactions on Affective Computing*, 2023.
- [41] T. Gao, X. Yao, and D. Chen, “Simcse: Simple contrastive learning of sentence embeddings,” in *EMNLP 2021-2021 Conference on Empirical Methods in Natural Language Processing, Proceedings*, 2021.
- [42] S.-w. Yang, P.-H. Chi, Y.-S. Chuang, C.-I. J. Lai, K. Lakhota, Y. Y. Lin, A. T. Liu, J. Shi, X. Chang, G.-T. Lin, *et al.*, “Superb: Speech processing universal performance benchmark,” *arXiv preprint arXiv:2105.01051*, 2021.
- [43] L. McInnes, J. Healy, N. Saul, and L. Großberger, “Umap: Uniform manifold approximation and projection,” *Journal of Open Source Software*, vol. 3, no. 29, p. 861, 2018.
- [44] M. I. Belghazi, A. Baratin, S. Rajeshwar, S. Ozair, Y. Bengio, A. Courville, and D. Hjelm, “Mutual information neural estimation,” in *International conference on machine learning*. PMLR, 2018, pp. 531–540.
- [45] B. C. Geiger, “On information plane analyses of neural network classifiers—a review,” *IEEE Transactions on Neural Networks and Learning Systems*, vol. 33, no. 12, pp. 7039–7051, 2021.
- [46] P. W. Koh and P. Liang, “Understanding black-box predictions via influence functions,” in *International conference on machine learning*. PMLR, 2017, pp. 1885–1894.
- [47] L. Arras, F. Horn, G. Montavon, K.-R. Müller, and W. Samek, “‘’ what is relevant in a text document?’: An interpretable machine learning approach,” *PLoS one*, vol. 12, no. 8, p. e0181142, 2017.
- [48] Z. Huang, J. Epps, D. Joachim, and V. Sethu, “Natural language processing methods for acoustic and landmark event-based features in speech-based depression detection,” *IEEE Journal of Selected Topics in Signal Processing*, vol. 14, no. 2, pp. 435–448, 2019.
- [49] G. S. Nathan, “The sounds of the world’s languages,” 1998.
- [50] J. R. Williamson, T. F. Quatieri, B. S. Helfer, R. Horwitz, B. Yu, and D. D. Mehta, “Vocal biomarkers of depression based on motor incoordination,” in *Proceedings of the 3rd ACM international workshop on Audio/visual emotion challenge*, 2013, pp. 41–48.
- [51] T. F. Quatieri and N. Malyska, “Vocal-source biomarkers for depression: A link to psychomotor activity,” in *Interspeech*, vol. 2, 2012, pp. 1059–1062.